

# Co-7% Ir Soft Magnetic Intermediate Layer for Perpendicular Media

Soyoung Park<sup>1,2</sup>, David E. Laughlin<sup>1,2,3</sup>, and Jian-Gang Zhu<sup>1,2,3</sup>, *Fellow, IEEE*

<sup>1</sup>Data Storage System Center, Carnegie Mellon University, Pittsburgh, PA 15213 USA

<sup>2</sup>Materials Science and Engineering Department, Carnegie Mellon University, Pittsburgh, PA 15213 USA

<sup>3</sup>Electrical Computer Engineering Department, Carnegie Mellon University, Pittsburgh, PA 15213 USA

**The current perpendicular magnetic recording (PMR) media uses a non-magnetic dual Ru intermediate layer. Replacing the bottom Ru layer with a Co-7at% Ir soft magnetic crystalline interlayer is expected to enhance both the magnetic field strength and gradient. Fabrication processing parameters were varied to develop the CoIr layer with desired properties (soft magnetic properties, texture, and dome morphology) to be utilized in practical PMR media design. First, the oxide was added to create a magnetically grain-to-grain isolated structure and the well segregated microstructure was obtained. Secondly, CoIr without the oxide was deposited on amorphous Ta and confirmed to have the hcp (00.2) texture and 5 nm Ru on top develops the hcp (00.2) texture epitaxially. The recording layer properties were not deteriorated with the replacement of Ru bottom layer with CoIr. The feasibility of CoIr application in the current PMR media will be discussed based on the experimental results.**

**Index Terms**—CoIr, soft magnetic intermediate layer, perpendicular thin film media.

## I. INTRODUCTION

**I**NCREASING the write field gradient should yield shaper transitions, reduce medium noise, and consequently enhance the signal-to-medium noise ratio [1]–[3]. This may be accomplished by replacing the non-magnetic intermediate layer with a soft magnetic layer in the current perpendicular thin film media, if the new intermediate layer also can serve the functions of the present intermediate layer. The present Ru intermediate layer consists of a dual layer structure: The bottom Ru layer (Ru<sup>Bottom</sup>) is usually deposited at low Ar pressure to produce a well oriented hcp (00.2) texture and the top Ru layer (Ru<sup>top</sup>) is deposited at high pressure to produce a dome morphology. It is not only the texture, but also the dome morphology that is crucial for producing the proper microstructure of the subsequently deposited granular magnetic layer [4]. To obtain a sufficiently narrow distribution of the c axis orientation for the hcp CoCrPt grains, a relatively thick bottom Ru layer has proven to be necessary [5]. In order to reduce the Ru IL thickness, Piramanayagam *et al.* introduced a crystalline SUL using CoFe and a magnetic intermediate layer using CoCr [6]. Choe *et al.* experimentally demonstrated a gain of the write field gradient and strength with the insertion of CoNiFe [2]. Although both of the above magnetic layers are hcp with lattice constants similar to that of CoCrPt magnetic layer, the associated intrinsic magnetocrystalline anisotropy makes them not ideal soft magnetic materials. Therefore, based on the work devised by Takahashi *et al.* [7], we have previously replaced the bottom Ru intermediate layer with a CoPt-CoIr bilayer structure with nearly zero net intrinsic anisotropy [8].

In this paper, we present experimental work on replacing the bottom Ru intermediate layer in current thin film media with a Co-7 at% Ir granular soft magnetic crystalline intermediate

layer. Co-7 at% Ir with the hcp structure (referred to as CoIr hereafter) has a zero magnetocrystalline anisotropy constant,  $K_1$  [9]. Hashimoto *et al.* studied CoIr alloys of different composition for application as a SUL [10]. The lattice mismatch with Ru is only 6.7%. Therefore, CoIr could be made magnetically soft and could be an excellent candidate for the replacement of the bottom Ru layer purpose. We assert that it is important to have the soft magnetic intermediate layer to be granular in nature in order to enhance the write field gradient. Magnetic softness arising from domain wall activities in continuous film will undoubtedly create a “blurred” imaging effect due to the intrinsic exchange length in the film which is usually significantly greater than the diameter of the grains. Here, CoIr-oxide films have been fabricated to create adequate granular microstructure with non-magnetic oxide grain boundaries. The sputtering processing parameters (use of seedlayer, Ar pressure, layer thickness, number of repeat for multilayer) were optimized for obtaining well oriented hcp (00.2) texture, dome top morphology, and soft magnetic properties. The feasibility of the granular CoIr to act as a novel intermediate layer was evaluated by its magnetic softness and the resulting magnetic and crystalline properties of the subsequently deposited CoPt layer.

## II. EXPERIMENTAL PROCEDURE

The films were deposited using a Leybold-Heraeus Z-400 sputtering system. The crystalline texture, segregated microstructure, and soft magnetic properties were optimized using process parameters, such as the Ar gas pressure and the thickness of each layer. A Co-7at% Ir alloy target was modified by adding SiO<sub>2</sub> chips depending on the need of oxide segregation. The film texture was quantified by x-ray diffraction (XRD)  $\theta$ - $2\theta$  scans and rocking curves of the hcp (00.2) peak. The microstructure was observed by transmission electron microscopy (TEM). DC demagnetization curves using an alternating field gradient magnetometer (AGM) was used to obtain the remnant coercivity ( $H_{cr}$ ) in order to evaluate the perpendicular anisotropy of the recording layer. M-H loops were taken using a vibrating sample magnetometer (VSM) in addition to AGM.

Manuscript received October 31, 2009; revised December 28, 2009; accepted January 30, 2010. Current version published May 19, 2010. Corresponding author: S. Park (e-mail: soyoung1@andrew.cmu.edu).

Color versions of one or more of the figures in this paper are available online at <http://ieeexplore.ieee.org>.

Digital Object Identifier 10.1109/TMAG.2010.2043231

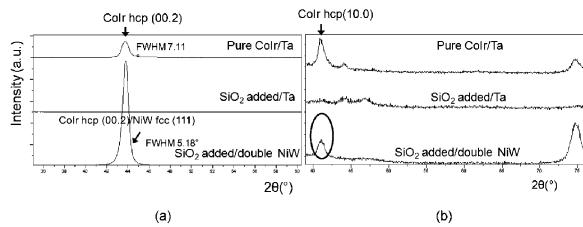


Fig. 1. XRD  $\theta$ - $2\theta$  scan showing that CoIr grows with (00.2) hcp texture with the help of NiW seedlayer. (a) Out of plane shows CoIr (00.2) peak is overlapped with NiW seedlayer peak that makes it difficult to identify CoIr texture. (b) In plane shows CoIr (10.0) peak, implying CoIr grows as hcp (00.2) texture in film co-sputtered with oxide.

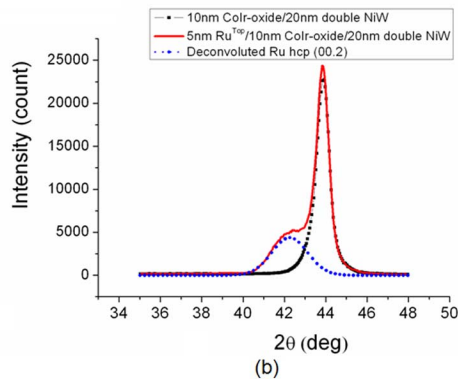
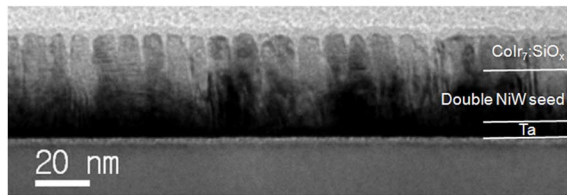


Fig. 2. (a) TEM cross section view showing that well segregated domed morphology was obtained in CoIr-oxide soft intermediate layer when 10 mT Ar pressure was used during the CoIr-oxide deposition. (b) XRD  $\theta$  -  $2\theta$  scan of CoIr-oxide/NiW seedlayer shown in (a) and 5 nm  $\text{Ru}^{\text{Top}}$  deposited on top of (a) stack.

### III. RESULTS AND DISCUSSION

#### A. Replacement of $\text{Ru}^{\text{Bottom}}$ With CoIr-Oxide Layer

First, 10 nm films of CoIr on Ta, CoIr-oxide on Ta, and CoIr-oxide on the NiW seedlayer were deposited to see if the desired texture could be developed. The XRD patterns in Fig. 1 confirm that the 10 nm CoIr layer on Ta has the hcp (00.2) texture. The addition of an oxide in order to create a granular structure impairs the crystallization; however, it was observed that an fcc (111) NiW double seedlayer underneath helped the metallic CoIr alloy to crystallize and the oxide to be segregated into the grain boundaries. The out of plane scan shows the CoIr (00.2) peak overlaps with the NiW seedlayer peak which makes it difficult to identify the CoIr texture. However, in plane scans show the CoIr (10.0) peak, demonstrating that CoIr grows with the hcp (00.2) texture in films co-sputtered with oxide.

Second, the Ar pressure during CoIr-oxide layer deposition was varied to achieve better texture and a well-segregated microstructure. The TEM cross section image [Fig. 2(a)] confirms that a well-segregated microstructure with uniform grain size

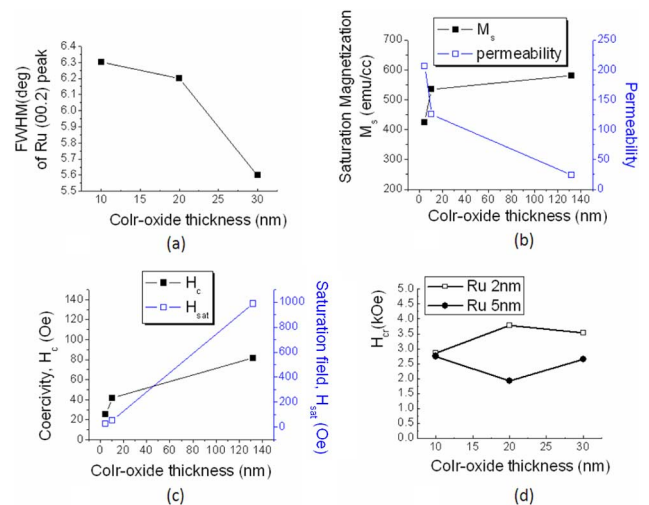


Fig. 3. (a) FWHM of an XRD rocking curve on 5 nm Ru (00.2) decreases with CoIr-oxide thickness. (b) The saturation magnetization increases and in plane permeability decreases as the CoIr-oxide grows thicker. (c) Increase of both in plane coercivity and saturation field taken from in plane MH hysteresis loop are consistent with the results in (b) that the CoIr-oxide becomes harder as it grows thicker. (d) The range of perpendicular  $H_{\text{cr}}$  of 14 nm CoPt-oxide recording layer on the CoIr-oxide stacks infers the perpendicular anisotropy was obtained with the 2 nm, 5 nm  $\text{Ru}^{\text{Top}}$ /CoIr-oxide/NiW seedlayer.

was achieved on top of the NiW seedlayer when it was deposited at low Ar pressure. After confirming the well segregated microstructure and the hcp (00.2) texture, 5 nm  $\text{Ru}^{\text{Top}}$  was deposited at different Ar pressures on the previously made CoIr-oxide stack. The XRD  $\theta$ - $2\theta$  scan in Fig. 2(b) showed when 10 mT Ar pressure was used during the 5 nm  $\text{Ru}^{\text{Top}}$  deposition, the film can epitaxially grow and has the best hcp (00.2) texture. The rocking curves of hcp (00.2) peaks shows that 10 nm CoIr-oxide/fcc (111) NiW seedlayer with FWHM  $5.7^\circ$  can induce 5 nm  $\text{Ru}^{\text{Top}}$  texture to have a FWHM of  $6.2^\circ$ .

Third, in order to further improve the texture, the thickness of the CoIr-oxide layer was varied and the fixed 5 nm  $\text{Ru}^{\text{Top}}$  was deposited at 10 mT Ar pressure. Fig. 3(a) shows a drop in the FWHM of  $\text{Ru}^{\text{Top}}$  (00.2) peak from  $6.3^\circ$  to  $5.6^\circ$  indicating that  $\text{Ru}^{\text{Top}}$  texture is improved as the CoIr-oxide thickness is increased. For the assessment of the magnetic properties, the saturation magnetization ( $M_s$ ) was measured from the in plane M-H initial curve and in plane permeability ( $\mu$ ) was extracted from the slope between the origin and 50% of the saturation magnetization. Fig. 3(b) shows that as the CoIr grows thicker,  $\mu$  decreases while  $M_s$  increases. The in plane hysteresis loops were consistent in that both  $H_c$  and  $H_{\text{sat}}$  increases as CoIr becomes thicker as shown in Fig. 3(c). It was concluded that the thicker CoIr-oxide layer becomes magnetically harder while the texture improves. Two reasons are speculated: 1) relatively more Ir-deficient regions where magneto crystalline  $K_1 > 0$  are present as it becomes thicker, or 2) the elongated shape of the columns as the CoIr-oxide grows thicker induces an effective shape anisotropy. To optimize the CoIr thickness, there is a tradeoff between good texture of  $\text{Ru}^{\text{Top}}$  and the magnetic softness. According to the reference [11], the range of the obtained permeability is satisfactory as the general SUL function only needs to be higher than 100. Only when the permeability is less than 100 does it start to degrade the write field gradient [11]. Also, [12] claims that if

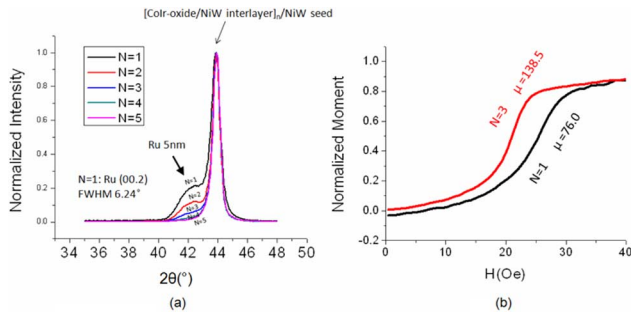


Fig. 4. The effect of lamination on  $\text{Ru}^{\text{TOP}}$  texture. (a) XRD  $\theta-2\theta$  scan after normalization of intensity with respect to the NiW fcc (111)/CoIr hcp (00.2) peak. Note that Ru peak disappears with the lamination.  $N$  is the number of laminate repetition. (b) In plane initial M-H curve showing permeability improves with the lamination.

the relative permeability is greater than 50, the readback signal is leveled off.

To have a rough grasp of how this developed stack ultimately affects on the properties of recording layer, the recording layer of 14 nm CoPt-oxide was deposited on the 2 nm, 5 nm  $\text{Ru}^{\text{TOP}}$ /CoIr-oxide/NiW stack. To evaluate the recording layer only, perpendicular DC demagnetization remnant curves were taken. It was experimentally confirmed that the CoIr-oxide soft intermediate layer does not contribute to the measurement. Therefore, the perpendicular remnant coercivity ( $H_{\text{cr}}$ ) defined as the coercivity of perpendicular DC demagnetization remnant curve is a quick measure of the perpendicular anisotropy of the recording layer. As shown in Fig. 3(d), there was no clear trend seen in  $H_{\text{cr}}$  but the range of  $H_{\text{cr}}$  infers that a perpendicular anisotropy was obtained with the varied CoIr-oxide thickness.

Fourth, the multilayer structure was devised and tried with 2 nm NiW interlayer in order to improve the texture even further. We found that the texture was worsened as the stack was repeated. Fig. 4(a) shows  $\text{Ru}^{\text{TOP}}$  hcp (00.2) peak disappears as the number of repeats is increased while the permeability significantly increases as shown in Fig. 4(b). It is believed that NiW interlayers make the structure magnetically soft in the plane because they break the exchange coupling along the thickness. However, the oxide in CoIr-oxide layer was not segregated well when laminated so that it appears to hinder the coherent epitaxial growth between NiW and CoIr-oxide.

In summary, it was proved that CoIr-oxide can have hcp (00.2) texture as well as well segregated microstructure. However, a sufficient  $c$  axis orientation requirement in CoIr-oxide stack has not yet been obtained despite various process optimization trials. This will lead to sacrifice the recording layer properties. Also, the additional need of a thick nonmagnetic NiW seedlayer can interrupt the magnetic flux closure between CoIr and the SUL. Therefore, in the next step, we removed the oxide in the CoIr layer aiming to improve the texture, to eliminate the additional NiW seedlayer, to increase  $M_s$ , and permeability for a better perfect imaging effect.

### B. Replacement of $\text{Ru}^{\text{Bottom}}$ With a CoIr Layer

Based on that observation that a CoIr layer can grow with the hcp (00.2) texture without any seedlayer as seen in Fig. 1, the part of conventional  $\text{Ru}^{\text{Bottom}}$  layer was replaced with pure

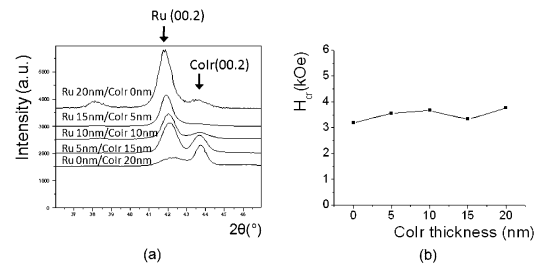


Fig. 5. (a) XRD  $\theta-2\theta$  scan showing both CoIr and Ru grow as hcp (00.2). (b) The perpendicular  $H_{\text{cr}}$  independence of CoIr thickness ( $x$ ) indicates the perpendicular anisotropy in the recording layer was not affected by replacement of part of  $\text{Ru}^{\text{Bottom}}$ .

CoIr keeping the total thickness 20 nm. 5 nm  $\text{Ru}^{\text{TOP}}$  was deposited at 30 mT on the stack with the different thickness ratios. Such dual- $\text{Ru}^{\text{TOP}}/(x \text{ nm } \text{Ru}^{\text{Bottom}} + (20 - x) \text{ nm } \text{CoIr}^{\text{Bottom}})$  stacks were examined by XRD  $\theta-2\theta$  scan as shown in Fig. 5(a). It was observed the CoIr grows with hcp (00.2) texture directly deposited on amorphous Ta and the  $\text{Ru}^{\text{TOP}}$  as thin as 5 nm epitaxially follows with hcp (00.2) texture. Rocking curves on Ru (00.4) peak show that constant FWHM in the range of 5–8° was obtained as the CoIr thickness ( $x$ ) is varied. A recording layer of 14 nm CoPt-oxide was deposited on the dual- $\text{Ru}^{\text{TOP}}/(x \text{ nm } \text{Ru}^{\text{Bottom}} + (20 - x) \text{ nm } \text{CoIr}^{\text{Bottom}})$  stack. Perpendicular  $H_{\text{cr}}$  of the recording layer in Fig. 5(b) also does not change with the varied CoIr thickness ( $x$ ). This indicates that perpendicular magneto anisotropy was not sacrificed by replacement of the  $\text{Ru}^{\text{Bottom}}$  layer. This is interpreted to mean that the replacement of  $\text{Ru}^{\text{Bottom}}$  with CoIr does not affect the crystallinity of the recording layer.

Another way to evaluate how the recording layer properties are affected by the insertion of CoIr is to obtain perpendicular M-H loops by VSM measurements. The slope was corrected by flattening the linear region from 70% of the maximum applied field. Fig. 6(a) is a reference for a conventional PMR design using a dual Ru IL. As mentioned earlier, 20 nm  $\text{Ru}^{\text{Bottom}}$  is deposited at low Ar pressure for the good texture and 5 nm or 20 nm  $\text{Ru}^{\text{TOP}}$  is deposited at high Ar pressure for the domed morphology. The  $\text{Ru}^{\text{TOP}}$  thickness was varied and the results show that thicker the  $\text{Ru}^{\text{TOP}}$ , higher the  $H_c$  and lower the  $\alpha$  (slope of the loop at  $H_c$  which is a measure of to the intergranular exchange coupling) were obtained. It is believed that the thicker  $\text{Ru}^{\text{TOP}}$  develops a better dome morphology, the better oxide segregation, and consequently, leads to better intergranular exchange decoupling and the higher perpendicular anisotropy. The corresponding TEM plan view image of CoPt-oxide/20 nm  $\text{Ru}^{\text{TOP}}/20 \text{ nm } \text{Ru}^{\text{Bottom}}/\text{Ta}$  showed that the oxide is clearly better segregated to the grain boundaries. Fig. 6(b) shows that 20 nm  $\text{Ru}^{\text{Bottom}}$  was replaced by 20 nm CoIr (FWHM 7.1°) layer and  $\text{Ru}^{\text{TOP}}$  thickness was varied. The same trend was shown in that the easy axis loop was obtained and the thicker  $\text{Ru}^{\text{TOP}}$  leads to the higher  $H_c$  and lower  $\alpha$  in the recording layer. However, the loop has a shoulder near zero field which can be attributed to the CoIr signal contribution. The information that we have in Fig. 6(b) is the summed CoPt-oxide recording layer and CoIr layer. Therefore, it is not valid to evaluate quantitatively the perpendicular magnetic

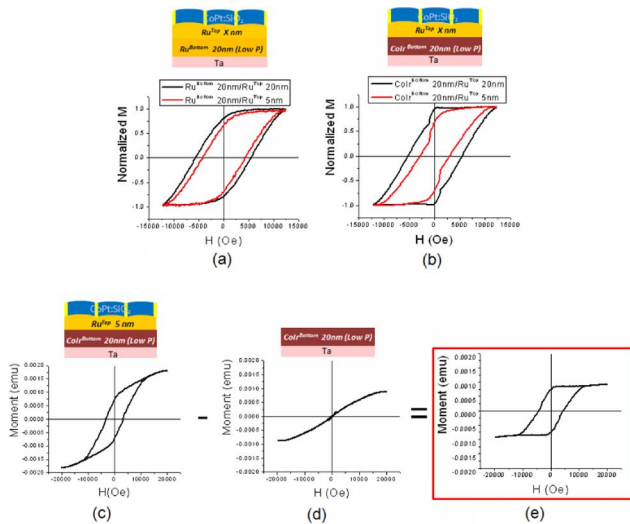


Fig. 6. Evaluation of the recording layer properties. VSM Perpendicular M-H Loop of (a) reference with double Ru IL and (b) the stack in which  $\text{Ru}^{\text{Bottom}}$  was replaced by  $\text{CoIr}^{\text{Bottom}}$ . (c)–(e) The procedure of extracting M-H loop of CoPt-oxide layer. The M-H loop of CoIr stack (d) was subtracted from that of the whole stack (c). The result (e) contains only the recording layer characteristic.

properties of CoPt-oxide-only film as evaluated in Fig. 6(a) with  $H_c$  or  $\alpha$ . In order to evaluate the recording layer properties only, perpendicular M-H loops were taken using the VSM for the CoPt-oxide/Ru/CoIr/Ta stack and the CoIr/Ta stack separately and subtracted the latter from the former data as illustrated in Fig. 6(c)–(e). It confirms that CoPt-oxide can have high perpendicular anisotropy ( $H_c \sim 4.5$  kOe) on this 5 nm  $\text{Ru}^{\text{Top}}/20$  nm  $\text{CoIr}^{\text{Bottom}}/\text{Ta}$  underlayer stack whereas the 5 nm  $\text{Ru}^{\text{Top}}/20$  nm  $\text{Ru}^{\text{Bottom}}/\text{Ta}$  underlayer stack can provide  $H_c \sim 4.3$  kOe. Also,  $\alpha$  does not change with the replacement of  $\text{Ru}^{\text{Bottom}}$  with  $\text{CoIr}^{\text{Bottom}}$ . This indicates that  $\text{CoIr}^{\text{Bottom}}$  does not harm  $\text{Ru}^{\text{Top}}$  to have good dome morphology, and the oxide segregates well in the recording layer as with double Ru IL. This demonstrates that Co-7%Ir layer can replace the part of Ru without a significant sacrifice of the texture or magnetic properties.

#### IV. CONCLUSION

A Co-7%Ir soft magnetic layer has been developed to replace a part of the Ru intermediate layer in the current perpendicular

thin film media. First, a well isolated, granular, hcp (00.2) textured CoIr-oxide was successfully developed with NiW seed-layer. Next, CoIr layer without oxide directly on an amorphous Ta layer was achieved to have good hcp (00.2) texture. With a 20 nm  $\text{CoIr}^{\text{Bottom}}$  layer and an additional 5 nm thin  $\text{Ru}^{\text{Top}}$ , the CoPt-oxide granular magnetic layer shows very similar texture and magnetic properties compared to the case of an optimized dual Ru intermediate layer. We conclude that CoIr is a good candidate to replace a major portion of the Ru IL in the current PMR media with potential advantages for improving the write field strength and gradient due to its soft magnetic nature and granular nano-structure. Further experimental studies will follow to demonstrate the recording performance gain, especially including comparison between designs with and without oxide.

#### ACKNOWLEDGMENT

This work was supported by the Data Storage Systems Center, and the Nanofabrication Facility at Carnegie Mellon University.

#### REFERENCES

- [1] K. Z. Gao, V. Sapozhnikov, A. Zheng, and O. Heinonen, *IEEE Trans. Magn.*, vol. 44, no. 11, p. 3400, 2008.
- [2] G. Choe, M. Minardi, K. Zhang, and M. Mirzamaani, *IEEE Trans. Magn.*, vol. 44, no. 11, p. 3480, 2008.
- [3] J.-G. Zhu, D. Z. Bai, and A. F. Torabi, *IEEE Trans. Magn.*, vol. 39, p. 1961, 2003.
- [4] T. Hikosaka, "Perpendicular magnetic recording medium and magnetic read/write apparatus," U.S. Patent 6,670,056 B2, Dec. 30, 2003.
- [5] J. Z. Shi, S. N. Piramanayagam, C. S. Mah, H. B. Zhao, J. M. Zhao, and Y. S. Kay, *Appl. Phys. Lett.*, vol. 87, no. 22, p. 222503, 2005.
- [6] S. N. Piramanayagam, J. Z. Shi, H. B. Zhao, C. S. Mah, J. R. Shi, J. M. Zhao, J. Zhang, and Y. S. Kay, *J. Magn. Magn. Mater.*, vol. 303, p. 287, 2006.
- [7] M. Takahashi, M. Tsunoda, and S. Saito, *J. Magn. Magn. Mater.*, vol. 321, p. 539, 2009.
- [8] S. Park, J.-G. Zhu, and D. E. Laughlin, *J. Appl. Phys.*, vol. 105, p. 07B723, 2009.
- [9] N. Kikuchi, O. Kitakami, S. Okamoto, Y. Shimada, A. Sakuma, Y. Otani, and K. Fukamichi, *J. Phys.: Condens. Matter*, vol. 11, no. 43, 1999.
- [10] A. Hashimoto, S. Saito, and M. Takahashi, *J. Magn. Soc. Jpn.*, vol. 30, p. 135, 2006.
- [11] S. Khizroev, Y. Liu, K. Mountfield, M. H. Kryder, and D. Litvinov, *J. Magn. Magn. Mater.*, vol. 246, no. 1–2, p. 335, 2002.
- [12] S. K. Khizroev, J. A. Bain, and M. H. Kryder, *IEEE Trans. Magn.*, vol. 33, no. 5, p. 2893, 1997.